

Recovery Temperature for Nonclassical Energy Transfer in Atom-Surface Scattering

B. Gumhalter,^{1,2} A. Šiber,² and J. P. Toennies³

¹The Abdus Salam International Centre for Theoretical Physics, Trieste, Italy

²Institute of Physics of the University, P.O. Box 304, 10001 Zagreb, Croatia

³Max-Planck-Institut für Strömungsforschung, D-37073 Göttingen, Germany

(Received 8 March 1999)

Nonperturbative expressions are derived for the angular resolved energy transfer spectra in the quantum regime of multiphonon scattering of inert gas atoms from surfaces. Application to He atom scattering from a prototype heat bath Xe/Cu(111) shows good agreement with experiments. This enables a full quantum calculation of the total energy transfer μ and from this the much debated recovery or equilibrium temperature T_r characteristic of zero energy transfer in gas-surface collisions in the free molecular flow regime. The classical universal character of μ and T_r is refuted.

PACS numbers: 68.35.Ja, 34.50.Dy, 47.45.Nd, 63.22.+m

Despite the great progress recently made in understanding the dynamics of gas-surface collisions [1], little effort has gone into applying this knowledge to problems of general relevance [2]. Because of their fundamental importance for a wide range of the flow phenomena [3], there is a need to be able to predict the magnitudes of the heat transfer μ [4] and the recovery temperature T_r at which zero energy transfer to the surface occurs in the free molecular flow regime [5], but the classically calculated μ and T_r generally fail to reproduce the experimental data [2]. However, the information on single-phonon and multiphonon excitations recently accumulated from He atom scattering (HAS) from surfaces [6–10] combined with novel theoretical developments now opens up the possibility of calculating the heat transfer on a microscopic level and in the fully quantum scattering regime. In this Letter a new approach based on multiphonon scattering theory [11–13] is developed to predict the energy transfer in interactions of He atom beams with Xe monolayers on Cu(111) which represent an ideal prototype heat bath encompassing both the dispersive and nondispersive surface phonons [10]. The calculations reproduce the HAS data remarkably well and thus enable a reliable prediction of the recovery temperature which is found to differ markedly from the results of classical accommodation theories currently in use [4,5].

The total energy transfer μ which enters the heat transfer and accommodation coefficients [2,4] is evaluated from

$$\mu(\mathbf{k}_i, T_s) = \int_{-\infty}^{\infty} \varepsilon N_{\mathbf{k}_i, T_s}(\varepsilon) d\varepsilon. \quad (1)$$

where $N_{\mathbf{k}_i, T_s}(\varepsilon)$ is the scattering spectrum which gives the probability density for an atom with initial momentum $\hbar\mathbf{k}_i$ to exchange energy ε with a surface at the temperature T_s . The final atom state can be either a continuum $|c\rangle$ or a bound state $|b\rangle$ of the static atom-surface potential $U(\mathbf{r})$ [14–16]. However, there are two major difficulties in applying Eq. (1) to atom-surface scattering. First, $N_{\mathbf{k}_i, T_s}(\varepsilon)$ and thereby $\mu(\mathbf{k}_i, T_s)$ are not directly

accessible in typical HAS time-of-flight (TOF) measurements from which most of the data are available at present. These experiments yield the *energy and angular resolved* quantities usually only for fixed total scattering angle $\theta_{SD} = \theta_i + \theta_f$, where θ_i (θ_f) is the initial (final) scattering angle. The TOF spectrum is directly proportional to the $c \rightarrow c$ component of the full energy and parallel momentum resolved scattering distribution $N_{\mathbf{k}_i, T_s}(\varepsilon, \Delta\mathbf{K})$ [13] which in turn is related to the *angular resolved* energy transfer

$$\mu_r(\mathbf{k}_i, T_s, \theta_f) = \frac{\int \varepsilon N_{\mathbf{k}_i, T_s}^{c \rightarrow c}(\varepsilon, \Delta\mathbf{K}(\varepsilon)) d\varepsilon}{\int N_{\mathbf{k}_i, T_s}^{c \rightarrow c}(\varepsilon, \Delta\mathbf{K}(\varepsilon)) d\varepsilon}. \quad (2)$$

As $\mu_r(\mathbf{k}_i, T_s, \theta_f)$ can be computed from both the theoretical $N_{\mathbf{k}_i, T_s}^{c \rightarrow c}(\varepsilon, \Delta\mathbf{K})$ and the experimental TOF spectra, a direct comparison of the two results enables the verification of model calculations. The second difficulty arises in calculations of the reliable multiphonon $N_{\mathbf{k}_i, T_s}(\varepsilon)$, obtained from $N_{\mathbf{k}_i, T_s}(\varepsilon, \Delta\mathbf{K})$ by integration over $\Delta\mathbf{K}$, in the regime in which it is important to treat the dynamics of both the projectile and surface vibrations quantum mechanically. However, the recent progress in interpreting the multiphonon HAS from monolayers of noble gas atoms (Ar, Kr, Xe) adsorbed on metals [7–10] makes it now possible to exactly calculate $N_{\mathbf{k}_i, T_s}(\varepsilon, \Delta\mathbf{K})$ and thereby assess the total energy transfer in the studied collisions. These adlayers sustain low-energy longitudinal (L) and shear-horizontal (SH) in-plane polarized modes with acousticlike dispersion and nondispersive vertically polarized Einstein-like modes (S). The presence of nondispersive modes gives rise to special interference effects in $N_{\mathbf{k}_i, T_s}(\varepsilon, \Delta\mathbf{K})$ which requires its calculation in a closed, nonperturbative form. Such a solution is presented below and applied to the study of energy transfer in HAS from $(\sqrt{3} \times \sqrt{3})R30^\circ$ monolayers of Xe on Cu(111) which exhibit very weak diffraction and hence can be considered as flat in energy exchange processes [10]. This suppresses selective adsorption assisted energy

transfer [15] and greatly simplifies calculations and comparisons of $N_{\mathbf{k}_i, T_s}^{c \rightarrow c}(\varepsilon, \Delta \mathbf{K})$ with the TOF spectra.

In the scattering regime in which uncorrelated phonon processes are dominant the angular resolved scattering spectrum has the following unitary form [11,12]:

$$N_{\mathbf{k}_i, T_s}(\varepsilon, \Delta \mathbf{K}) = \int_{-\infty}^{\infty} \frac{d\tau d^2 \mathbf{R}}{(2\pi\hbar)^3} e^{i[\varepsilon\tau - \hbar(\Delta \mathbf{K})\mathbf{R}]/\hbar} \times \exp[2W(\tau, \mathbf{R}) - 2W]. \quad (3)$$

Here $2W(\tau, \mathbf{R})$ is the scattering function [12], $2W = 2W(\tau = 0, \mathbf{R} = 0)$ is the exponent of the Debye-Waller factor (DWF) [17], and τ and \mathbf{R} are auxiliary integration variables used to project the states with ε and $\Delta \mathbf{K}$ from the integral on the right-hand side of Eq. (3). In the range of validity of Eq. (3) the energy and parallel momentum are conserved in each phonon exchange process and ε and $\Delta \mathbf{K}$ are constrained to satisfy the total energy and parallel momentum conservation in the collision. Using expression (3), it is possible to write Eq. (1) as

$$\mu(\mathbf{k}_i, T_s) = i \frac{\partial}{\partial \tau} 2W(\tau = 0, \mathbf{R} = 0), \quad (4)$$

which can be readily calculated once $2W(\tau, \mathbf{R})$ is established. In the following the projectile-phonon coupling is assumed linear in the adsorbate displacements since this gives the dominant multiphonon contribution observed in HAS [18]. This yields [12]

$$2W(\tau, \mathbf{R}) = \sum_{\mathbf{Q}, \mathbf{G}, j, k_z} [|\mathcal{V}_{k_z, k_{zi}, j}^{\mathbf{K}_i, \mathbf{Q}+\mathbf{G}}(+)|^2 [\bar{n}(\omega_{\mathbf{Q}j}) + 1] \times e^{-i[\omega_{\mathbf{Q}j}\tau - (\mathbf{Q}+\mathbf{G})\mathbf{R}]} + |\mathcal{V}_{k_z, k_{zi}, j}^{\mathbf{K}_i, \mathbf{Q}+\mathbf{G}}(-)|^2 \bar{n}(\omega_{\mathbf{Q}j}) e^{i[\omega_{\mathbf{Q}j}\tau - (\mathbf{Q}+\mathbf{G})\mathbf{R}]}], \quad (5)$$

where \mathbf{Q} , j , and $\omega_{\mathbf{Q}j}$ denote the parallel wave vector, branch index, and frequency of a normal phonon mode, respectively, and \mathbf{G} is the adlayer reciprocal lattice vector. $\mathbf{k} = (\mathbf{K}, k_z)$, where k_z is the quantum number describing projectile perpendicular motion in c or b

states of $U(\mathbf{r})$. $\bar{n}(\omega_{\mathbf{Q}j})$ is the Bose-Einstein distribution, and $\mathcal{V}_{k_z, k_{zi}, j}^{\mathbf{K}_i, \mathbf{Q}+\mathbf{G}}(\pm)$ denote one-phonon emission (+) and absorption (-) on-shell scattering matrix elements normalized to particle current in the z direction [10,12]. Substitution of expression (5) into (4) gives

$$\mu(\mathbf{k}_i, T_s) = \mu_0(\mathbf{k}_i) + \mu_{\text{rec}}(\mathbf{k}_i, T_s), \quad (6)$$

in which the temperature-independent part is

$$\mu_0(\mathbf{k}_i) = \sum_{\mathbf{Q}, \mathbf{G}, j, k_z} \hbar \omega_{\mathbf{Q}j} |\mathcal{V}_{k_z, k_{zi}, j}^{\mathbf{K}_i, \mathbf{Q}+\mathbf{G}}(+)|^2, \quad (7)$$

and the T_s dependence is determined by the recoil term

$$\mu_{\text{rec}}(\mathbf{k}_i, T_s) = \sum_{\mathbf{Q}, \mathbf{G}, j, k_z} \hbar \omega_{\mathbf{Q}j} [|\mathcal{V}_{k_z, k_{zi}, j}^{\mathbf{K}_i, \mathbf{Q}+\mathbf{G}}(+)|^2 - |\mathcal{V}_{k_z, k_{zi}, j}^{\mathbf{K}_i, \mathbf{Q}+\mathbf{G}}(-)|^2] \bar{n}(\omega_{\mathbf{Q}j}), \quad (8)$$

which vanishes in the recoilless trajectory approximation (TA) for the projectile motion [19]. However, the TA may fail even for heavier atoms [16,20], and in the present quantum scattering regime the recoil is large (c.f. Figs. 10 and 11 in Ref. [10]) making $\mu(\mathbf{k}_i, T_s)$ strongly T_s dependent.

The nonperturbative multiphonon solution for $N_{\mathbf{k}_i, T_s}(\varepsilon, \Delta \mathbf{K})$, which enables explicit calculation of expression (2) and thus a direct comparison with the HAS data, is obtained by separating the most strongly coupling Einstein branch $j = S$ of frequency ω_S out of the sum in Eq. (5), giving

$$\exp[2W(\tau, \mathbf{R}) - 2W] = N_{\mathbf{k}_i, T_s}^{\text{Ein}}(\tau, \mathbf{R}) N_{\mathbf{k}_i, T_s}^{\text{dis}}(\tau, \mathbf{R}), \quad (9)$$

where dis denotes the remaining dispersive modes. Employing trigonometric identities to $N_{\mathbf{k}_i, T_s}^{\text{Ein}}(\tau, \mathbf{R})$ yields

$$N_{\mathbf{k}_i, T_s}^{\text{Ein}}(\tau, \mathbf{R}) = e^{-2W_S} \sum_{l=-\infty}^{\infty} P_l(\mathbf{R}) e^{-il\omega_S\tau}, \quad (10)$$

where $2W_S = 2W_S(\tau = 0, \mathbf{R} = \mathbf{0})$ is the corresponding Debye-Waller exponent and

$$P_l(\mathbf{R}) = \left[\left(\frac{[\bar{n}(\omega_S) + 1] \mathcal{V}_S^2(\mathbf{R}, +)}{\bar{n}(\omega_S) \mathcal{V}_S^2(\mathbf{R}, -)} \right)^l I_l(\sqrt{4\bar{n}(\omega_S) [\bar{n}(\omega_S) + 1] \mathcal{V}_S^2(\mathbf{R}, +) \mathcal{V}_S^2(\mathbf{R}, -)}) \right], \quad (11)$$

where $\mathcal{V}_S^2(\mathbf{R}, \pm) = \sum_{\mathbf{Q}, \mathbf{G}, k_z} |\mathcal{V}_{k_z, k_{zi}, S}^{\mathbf{K}_i, \mathbf{Q}+\mathbf{G}}(\pm)|^2 \times e^{\mp i[\omega_S\tau - (\mathbf{Q}+\mathbf{G})\mathbf{R}]}$ and I_l is the modified Bessel function of the first kind. Hence, the separated Einstein phonon component of the spectrum in Eq. (3) takes the form

$$N_{\mathbf{k}_i, T_s}^{\text{Ein}}(\varepsilon, \Delta \mathbf{K}) = e^{-2W_S} \sum_{l=-\infty}^{\infty} N_l(\Delta \mathbf{K}) \delta(\varepsilon - l\hbar\omega_S), \quad (12)$$

where $N_l(\Delta \mathbf{K}) = \int d^2 \mathbf{R} e^{-i(\Delta \mathbf{K})\mathbf{R}} P_l(\mathbf{R}) / (2\pi)^2$ is the intensity of the l th Einstein multiphonon loss ($l > 0$)

or gain ($l < 0$) peak. The elastic intensity $N_{\mathbf{k}_i, T_s}^{\text{Ein}}(\varepsilon = 0, \Delta \mathbf{K} \neq \mathbf{0})$ is nonvanishing for $T_s > 0$ because multiple exchange of nondispersive phonons may give rise to finite momentum transfer without a net energy transfer. However, the spectral intensity of the specular elastic peak is $e^{-2W_S} \delta(\Delta \mathbf{K})$ because $P_0(\mathbf{R} \rightarrow \infty) \rightarrow 1$. On the other hand, the elastic peak in $N_{\mathbf{k}_i, T_s}(\varepsilon)$, obtained from Eq. (12) by integrating over all $\Delta \mathbf{K}$, is weighed by $e^{-2W_S} P_0(\mathbf{R} = \mathbf{0})$ but with $P_0(\mathbf{R} = \mathbf{0}) \neq 1$ due to the same multiquantum exchange effect.

A similar procedure yields for $N_{\mathbf{k}_i, T_s}^{\text{dis}}(\tau, \mathbf{R})$ in Eq. (9):

$$N_{\mathbf{k}_i, T_s}^{\text{dis}}(\tau, \mathbf{R}) = e^{-2W_{\text{dis}}} \exp \left[\sum_{\mathbf{Q}, \mathbf{G}, k'_z, j \neq S} \sqrt{4[\bar{n}(\omega_{\mathbf{Q}j}) + 1]\bar{n}(\omega_{\mathbf{Q}j})} |\mathcal{V}_{k'_z, k_{zi}, j}^{\mathbf{K}_i, \mathbf{Q}+\mathbf{G}}(+)|^2 |\mathcal{V}_{k'_z, k_{zi}, j}^{\mathbf{K}_i, \mathbf{Q}+\mathbf{G}}(-)|^2 \right. \\ \left. \times \cos \left(i \ln \sqrt{\frac{[\bar{n}(\omega_{\mathbf{Q}j}) + 1] |\mathcal{V}_{k'_z, k_{zi}, j}^{\mathbf{K}_i, \mathbf{Q}+\mathbf{G}}(+)|^2}{\bar{n}(\omega_{\mathbf{Q}j}) |\mathcal{V}_{k'_z, k_{zi}, j}^{\mathbf{K}_i, \mathbf{Q}+\mathbf{G}}(-)|^2}} + [\omega_{\mathbf{Q}j}\tau - (\mathbf{Q} + \mathbf{G})\mathbf{R}] \right) \right]. \quad (13)$$

Expressions (10)–(13) are *exact* within the validity of (3) [12] and include the *combined effect of recoil and temperature* on the multiphonon scattering spectra.

The calculations of expressions (5)–(13) were carried out by modeling $U(\mathbf{r}) = U(z)$, the projectile-phonon coupling and the dynamical matrix of the Xe monolayer and 40 layer thick Cu(111) slab as in Refs. [9,10]. The calculated $N_{\mathbf{k}_i, T_s}^{\text{dis}}(\varepsilon, \Delta \mathbf{K})$ and $\mu_r(\mathbf{k}_i, T_s, \theta_f)$ in the multiphonon scattering regime were tested by directly comparing with experiment. Figure 1 shows a comparison of the angular resolved energy transfer obtained from Eq. (2) without invoking any fit parameters, with the values calculated by integrating the TOF spectra for fixed θ_{SD} [9,10]. The inset shows a comparison of the experimental and calculated scattering spectrum (3) for one particular set of the scattering parameters. Thus confirmed consistency of the theoretical with experimental results enables consistent calculation of $\mu(\mathbf{k}_i, T_s)$.

Figure 2 shows the temperature dependence of total heat transfer in HAS from Xe/Cu(111) normalized to the vertical component of the projectile incident energy, $E_{zi} = E_i \cos^2 \theta_i$. The T_s dependence of $\mu_{\text{rec}}(\mathbf{k}_i, T_s)$

hinders energy transfer to phonons and causes negative slopes in the plots. This arises from a larger phase space for projectile $c \rightarrow c$ transitions into final states with $E_z > E_{zi}$. There it may give rise to negative $\mu(\mathbf{k}_i, T_s)$ (e.g., for $E_i = 2.4$ meV and $\theta_i = 50^\circ$ at $T_s > 62$ K) and hence to the heating of the scattered beam. In the classical theory this effect is independent of the accommodation coefficient and hence of θ_i [5]. Here, the universal behavior of $\mu(\mathbf{k}_i, T_s)$ for higher E_i , as exemplified by the near coincidence of the two highest energy curves in Fig. 2 and confirmed by additional calculations at high E_i , manifests itself only for *fixed* θ_i because the θ_i dependence of three-dimensional scattering matrix elements is not contained solely in the factorizable scaling factor E_{zi} [10,12]. Also, extension of the classical Baule expression pertinent to energy transfer in the cube model ($\Delta \mathbf{K} = 0$) to quantum surface scattering [19] is generally inadequate, as is demonstrated in comparison with our results for $T_s = 0$. Since $U(z)$ with the well depth of 6.6 meV supports three bound states we show in the inset

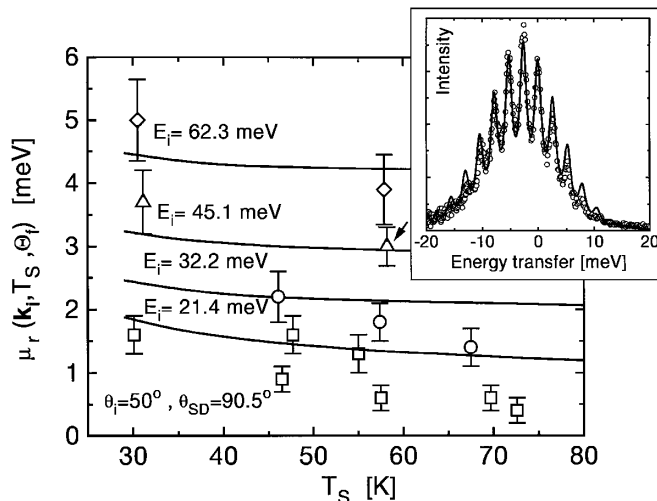


FIG. 1. Comparison of the temperature dependence of the *angular resolved* energy transfer $\mu_r(\mathbf{k}_i, T_s, \theta_f)$ calculated from He \rightarrow Xe/Cu(111) TOF spectra for four experimental E_i and fixed scattering geometry (open symbols), and from the present model (solid lines). The inset shows a comparison of the measured and calculated multiphonon scattering spectrum for $E_i = 45.11$ meV, $\theta_i = 50^\circ$, $T_s = 58.2$ K.

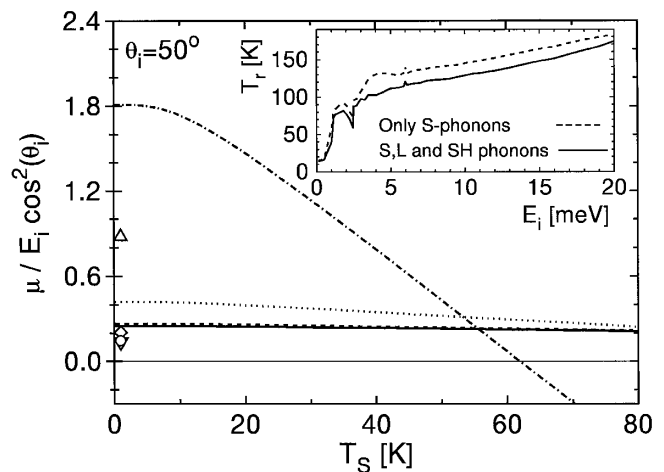


FIG. 2. Temperature dependence of the total energy transfer μ in He \rightarrow Xe/Cu(111) collisions normalized to E_{zi} for $\theta_i = 50^\circ$ and $E_i = 80$ meV (solid curve), 60 meV (long-dashed curve), 20 meV (short-dashed curve), and 2.4 meV (dashed-dotted curve). The corresponding normalized values of μ at $T_s = 0$ obtained from the Baule formula corrected for the well depth are denoted by the inverted triangle, circle, diamond and triangle, respectively. The scattered beam is heated on the average if $\mu < 0$. Inset: relative contributions of the phonon modes to the recovery temperature T_r (see text).

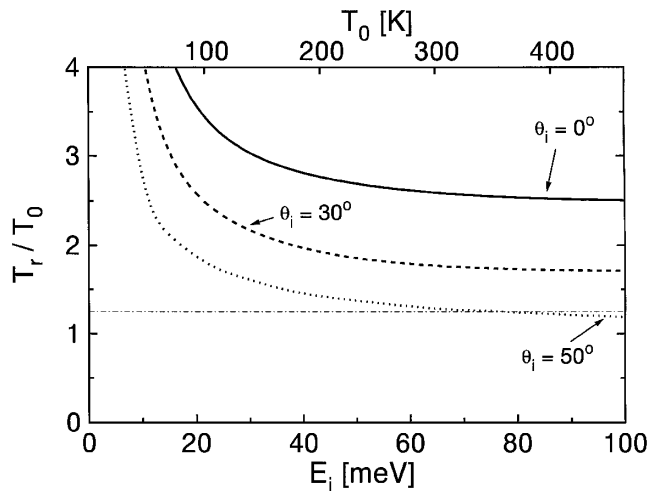


FIG. 3. Recovery factor T_r/T_0 for a prototype heat bath sustaining phonon modes typical of Xe/Cu(111) system plotted as a function of the incident energy E_i or stagnation temperature T_0 of the gas for three representative incident angles θ_i . Dashed-dotted line is the classical result $T_r/T_0 = 1.25$.

the low- E_i dependence of the recovery temperature [for which $\mu(\mathbf{k}_i, T_r) = 0$] calculated for the present phonon heat bath for fixed θ_i , for He coupling either only to S- or to S-, L-, and SH-phonon modes. The small difference indicates that the major contribution is from strong He atom coupling to vertically polarized S modes [10]. Rapid variations in T_r are caused by kinematic focusing in S-phonon assisted $c \rightarrow b$ transitions for large parallel momentum transfer.

For monoatomic gases the standard classical accommodation theory gives $T_r = E_i/2k_B$ and, to a good approximation, $E_i \approx 5k_B T_0/2$, where T_0 is the stagnation temperature of beam gas prior to expansion in the nozzle [2]. This yields the recovery factor $T_r/T_0 \approx 1.25$ but deviations from this universal behavior have been observed in wind tunnel molecular beam experiments [2] and their explanation was proposed in terms of heuristically modified classical expressions [5]. The present quantum theory enables essential progress beyond the classical results by allowing the parallel momentum exchange with phonons, multiphonon interference, and quantum recoil of the projectile. Their interplay gives the recovery factor as a function of E_i (or T_0) and θ_i which for our prototype heat bath is shown in Fig. 3. Quite generally, T_r is largest for normal incidence and only at higher E_i (i.e., T_0) quantum results may approach the classical limit so far observed only for rough technical surfaces [2]. Large deviations from the classical limit at low E_i are due to the quantum regime which allows larger $\Delta\mathbf{K}$ and transitions affected by the bound states of He-surface potential. Qualitatively, these findings are not system specific as the present theory is quite general and can be readily extended to calculations of the heat transfer in collisions of He [21,22] or heavier rare gas atoms [16,23] with clean surfaces in a wide range of scattering conditions.

In summary, we have shown that in inelastic gas-surface scattering under the conditions of free molecular flow the combination of quantum and temperature effects gives rise to a violation of the universality of the energy transfer and recovery factor predicted by the classical accommodation theory.

The work in Zagreb was supported in part by NSF Grant No. JF-133.

- [1] See the articles in *Helium Atom Scattering from Surfaces*, edited by E. Hulpke, Springer Series in Surface Sciences Vol. 27 (Springer, Berlin, 1992).
- [2] H. Legge, J.P. Toennies, and J. Lüdecke in *Rarefied Gas Dynamics 19*, edited by J. Harvey and G. Lord (Oxford Science Publications, New York, 1994), Vol. II, p. 988; J.P. Toennies, *ibid.*, p. 921; H. Legge, J.R. Manson, and J.P. Toennies, *J. Chem. Phys.* **110**, 8767 (1999).
- [3] G.A. Bird *Molecular Gas Dynamics* (Clarendon Press, Oxford, 1976).
- [4] S.A. Schaaf and P.L. Chambré *Flow of Rarefied Gases* (Princeton University Press, Princeton, New Jersey, 1961).
- [5] C. Cercignani and M. Lampis, *J. Appl. Math. Phys.* **27**, 733 (1976).
- [6] F. Hofmann, J.P. Toennies, and J.R. Manson, *J. Chem. Phys.* **106**, 1234 (1997).
- [7] K.D. Gibson and S.J. Sibener, *Phys. Rev. Lett.* **55**, 1514 (1985).
- [8] C. Ramseyer, V. Pouthier, C. Girardet, P. Zeppenfeld, M. Büchel, V. Diercks, and G. Comsa, *Phys. Rev. B* **55**, 13 203 (1997); A.P. Graham, M.F. Bertino, F. Hofmann, J.P. Toennies, and Ch. Wöll, *J. Chem. Phys.* **106**, 6194 (1997).
- [9] J. Braun, D. Fuhrmann, A. Šiber, B. Gumhalter, and Ch. Wöll, *Phys. Rev. Lett.* **80**, 125 (1998).
- [10] A. Šiber, B. Gumhalter, J. Braun, A.P. Graham, M.F. Bertino, J.P. Toennies, D. Fuhrmann, and Ch. Wöll, *Phys. Rev. B* **59**, 5898 (1999).
- [11] K. Burke, B. Gumhalter, and D.C. Langreth, *Phys. Rev. B* **47**, 12 852 (1993).
- [12] A. Bilić and B. Gumhalter, *Phys. Rev. B* **52**, 12 307 (1995).
- [13] B. Gumhalter and A. Bilić, *Surf. Sci.* **370**, 47 (1997).
- [14] J. Böheim and W. Brenig, *Z. Phys. B* **41**, 243 (1981); T. Brunner and W. Brenig, *Surf. Sci.* **291**, 192 (1993).
- [15] J. Böheim, *Surf. Sci.* **148**, 463 (1984).
- [16] A. Šiber and B. Gumhalter, *Phys. Rev. Lett.* **81**, 1742 (1998).
- [17] B. Gumhalter, *Surf. Sci.* **347**, 237 (1996).
- [18] G. Armand and J.R. Manson, *Phys. Rev. Lett.* **53**, 1112 (1984); *ibid.* *Surf. Sci.* **195**, 513 (1988).
- [19] V. Celli, D. Himes, P. Tran, J.P. Toennies, Ch. Wöll, and G. Zhang, *Phys. Rev. Lett.* **66**, 3160 (1991).
- [20] C.A. DiRubio, D.M. Goodstein, B.H. Cooper, and K. Burke, *Phys. Rev. Lett.* **73**, 2768 (1994).
- [21] A. Šiber and B. Gumhalter, *Surf. Sci.* **385**, 270 (1997).
- [22] A. Šiber, B. Gumhalter, and J.P. Toennies, *Vacuum* **54**, 315 (1999).
- [23] F. Althoff, T. Andersson, and S. Andersson, *Phys. Rev. Lett.* **79**, 4429 (1997).